forests

MDPI

Article

Measuring Distances and Areas under Forest Canopy Conditions—A Comparison of Handheld Mobile Laser Scanner and Handheld Global Navigation Satellite System

Petru Tudor Stăncioiu [1,*], Ioan Dutcă [1,2], Sergiu Constantin Florea [1,3] and Marius Paraschiv [4]

[1] Department of Silviculture, Faculty of Silviculture and Forest Engineering, Transilvania University of Brasov, Șirul Beethoven 1, 500123 Brașov, Romania
[2] Department of Sustainability, Buckinghamshire New University, Queen Alexandra Rd., High Wycombe HP11 2JZ, UK
[3] Forest Design SRL, Nicovalei No. 33, 500473 Brașov, Romania
[4] National Institute for Research and Development in Forestry, "Marin Drăcea", Cloșca Street 13, 500040 Brașov, Romania
* Correspondence: petru.stancioiu@unitbv.ro

Abstract: Measuring distances and areas under forest canopy conditions is often required for a broad range of forest research and management-related activities. While modern technologies, such as handheld mobile laser scanning (MLS), made possible the tridimensional representation of forests with great accuracy, the practical application is still limited by its high costs and challenging data processing. The handheld Global Navigation Satellite System (GNSS) represents the classical alternative, determining the distances and areas based on point coordinates. In this study, we aimed to assess the accuracy of a handheld GNSS, relative to the handheld MLS, in measuring distances and areas under forest canopy conditions. The material consists of 209 ant nests, which were mapped in a mixed-species deciduous forest of North-Eastern Romania. The GNSS- and MLS-based distances among nests were compared using the Bland–Altman plots. The differences in size and shape of the areas described by the nests were analyzed using (i) the shape compactness and (ii) the form factor of the convex polygons. In general, the GNSS-based distances were shorter compared with those based on MLS. However, for most cases, the intervals of agreement between the two instruments were within the limits of GNSS accuracy (i.e., ±10 m). The largest mean differences occurred when nests were in dense canopy conditions and on rugged terrain. The GNSS-based area of the convex polygons was smaller in most cases, but no significant correlation between the size of the area and the size of the relative difference was found. Furthermore, both the shape compactness and the form factor of the polygons were also smaller for the GNSS-based method compared with the MLS-based method, with differences up to 10%. In conclusion, measurements recorded by GNSS were less accurate, and under certain forest conditions (dense canopies, rugged terrain), large systematic errors can occur and therefore limit its use.

Keywords: handheld GNSS; handheld MLS; spatial analysis; Bland–Altman; bias; accuracy; canopy density; ant nests

Citation: Stăncioiu, P.T.; Dutcă, I.; Florea, S.C.; Paraschiv, M. Measuring Distances and Areas under Forest Canopy Conditions—A Comparison of Handheld Mobile Laser Scanner and Handheld Global Navigation Satellite System. *Forests* **2022**, *13*, 1893. https://doi.org/10.3390/f13111893

Academic Editors: Paul Sestras, Ștefan Bilașco, Mihai Nita and Sanda Roșca

Received: 6 October 2022
Accepted: 7 November 2022
Published: 11 November 2022

1. Introduction

Characterization of forested landscapes is usually based on field samples, and therefore, the uncertainty of the measurements carried out at the sample level becomes very important [1]. The uncertainty at the landscape level depends on both the sample size and the measurement uncertainty at the level of individual observations. However, in forestry, since most parameters of interest are expressed per unit of forest area, measuring distances and areas is routinely used in forestry sampling. In obtaining accurate and precise forestry-based estimates, increasing the sample size can increase the costs to unacceptable

levels; therefore, compromises should be made between increasing the sample size and reducing the uncertainty at the individual observation level.

Modern technology, such as airborne laser scanning (ALS) and terrestrial mobile laser scanning (MLS), has tremendously improved our ability to assess natural resources over large areas not only due to the improved accuracy of some classic tree measurements (diameter, height) but also due to allowing for measuring other parameters (leaf area index [2], gap fraction [3], canopy radiation [4], crown structure [5], branch structure [6], biomass [7], stem form [8]) much more difficult or impossible to assess with traditional methods. It also allows for a faster data acquisition process [1] and automated processing afterward. Therefore, these new technologies can be used in a wide array of forest-related studies.

Deciphering spatial patterns helps the understanding of ecological processes [9], making spatial analyses very common in research, monitoring, and management of natural resources, including plants [10–13] and also diverse animal taxa, such as insects [14], spiders [15], mammals, reptiles [11], and birds [11,16]. However, for an accurate interpretation, the study of forest-related patterns (e.g., clumping) and processes (e.g., competition) relies on accurate spatial coordinates. As MLS is using a laser beam to measure distances and angles to objects around the scanner, the resulting point cloud allows for scanned object positioning as well. Thus, this technology, besides offering an accurate measurement for all parameters mentioned before, can also produce location information [17]. However, despite its accuracy, the location information is not georeferenced (does not bear geographical information) as data obtained by classic receptors using the Global Navigation Satellite System (GNSS). On the other hand, the latter is affected by unfavorable conditions, which limit signal quality [18] and, therefore, its utility in some natural conditions. Forest stand canopies (many times closed and dense) are an important condition that hinders GNSS signal reception, making it less efficient [19,20]. Additionally, tree density [21] and other factors, such as terrain configuration [22], collection time (i.e., ensuring enough number of position fixes per point), and satellite geometry, could also affect the accuracy of GNSS instruments [23]. Therefore, when higher spatial accuracy is needed, this technology is less applicable. Although some devices have the ability to average more samples for a location and, therefore, reach better accuracy, the time needed for this is rather long and is not feasible for day-by-day measurements in forestry use.

Despite these disadvantages, handheld GNSS technology is still widely used in research and management activities. Their lower cost and the fact that they are still more user-friendly (in terms of data collection and further processing) make them an appropriate choice for expediting field activities, especially when larger errors (e.g., a few meters) are accepted [22]. One of the pattern analyses used in ecology refers to finding the attraction or deterrence of a certain species towards some habitat features. For example, for red wood ants (*Formica* spp.), many environmental variables were considered to influence habitat suitability, such as stand canopy cover [24], forest edge [25], tree species [26,27], insolation [28], and forest fragmentation [29]. More recently, underground gases reaching the surface were shown to encourage site selection of ants [30].

Taking into account all of the above, the accuracy of determining the spatial position of nests compared with such habitat features becomes important. However, as mentioned before, besides accuracy, instrument price and time costs are influencing the choice of appropriate tools. The present study aimed to compare the positioning accuracy in forest conditions of two different instruments: a low-cost classic handheld GNSS (GPSMap 60CSx, Garmin Ltd., Olathe, KS, USA) and a more expensive mobile laser scanner (GeoSLAM-ZebRevo, GeoSLAM Ltd., Nottingham, UK). The dataset used for this analysis consisted of forest anthills from two separate experimental areas.

2. Materials and Methods

2.1. Study Site

Research was conducted in a mixed deciduous species forest located on a hilly region near the town of Pașcani (Iași County, northeastern part of Romania; Figure 1). Altitudes range from 280 to 300 m a.s.l., slopes are between 0 and 20 degrees, and the aspects are mostly sunny (S, S-E, S-W, E, W- [31]). The mean annual temperature is 8.4 °C, and the mean annual precipitation is 559 mm [32].

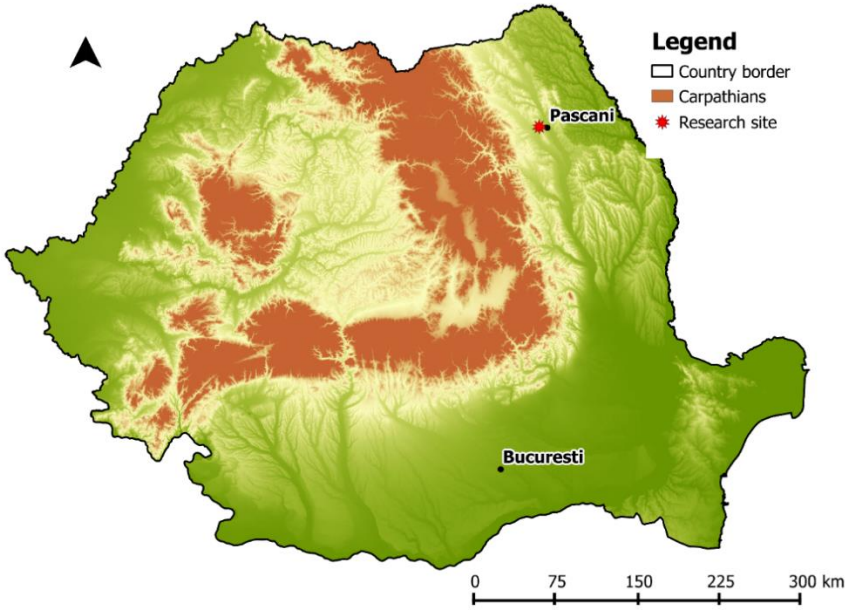

Figure 1. Location of research site.

To cover various conditions (in terms of crown cover, tree species composition, and terrain configuration), two distinct sites were chosen for the experiment, each of them hosting a colony of red wood ants (*Formica* spp.):

- Site 1—with 120 ant nests across three different stands (covering altogether 36.5 ha) with ages ranging between 50 and 70 years, dominated by oaks (sessile oak, *Quercus petraea* (Matt.) Liebl., and pedunculate oak, *Q. robur* L.). Scattered trees of hornbeam (*Carpinus betulus* L.), European beech (*Fagus sylvatica* L.), and wild cherry (*Prunus avium* L.) were present as well [31].
- Site 2—with 89 ant nests across five different stands (covering altogether 48.2 ha) with ages ranging between 30 and 55 years, dominated by oaks (sessile oak and pedunculate oak), hornbeam, and European beech. Wild cherry, sycamore (*Acer pseudoplatanus* L.), and trembling aspen (*Populus tremula* L.) were present but in low numbers (scattered trees) [31].

Stand canopies in the two sites were quite closed (between 80% and 100% [31]). Tree species distribution was heterogeneous and sometimes patchy. The terrain was generally flat, but some ravines were also present in Site 1.

2.2. Methods

Before starting to collect location information, the ant nests were inventoried, and each nest was coded, a red flag containing the nest code being placed at the tip of the nest. The code was also recorded on the closest tree with paint spray. The location for each nest was recorded with a handheld GNSS (Garmin GPSMap 60CSx; Figure A1) with an accuracy up to 10 m [33]. The position was recorded at the tip of the red flag (nests were inventoried in ascending order of the numbers assigned). Before the inventory with the mobile laser scanner (MLS), the two ant nest colonies, which are rather large and cover long distances,

were divided into seven separate sets (four in Site 1 and three in Site 2). This separation was needed to ensure that scanning sessions were shorter than 25 min, to avoid producing very large point cloud data sets (which in turn would hinder the later data processing). The number of nests in a set ranged between 14 and 40. Next, each of the seven sets was scanned (in ascending order of the ant nest number) using a GeoSLAM-Zeb-Revo (GeoSLAM Ltd., Nottingham, UK) mobile handheld laser scanner with a relative accuracy up to 3 cm [34] (Figure A1). Before the initiation of scanning, a starting point was temporarily marked in the field by placing on a flat ground the scanner backpack. To complete the survey, the user returned to the starting point, and the scanner was positioned in approximately the same position used for initialization [35]. This was necessary to ensure that the collected data can be successfully processed into a 3D point cloud later [36]. For good-quality MLS data, the operator walked around each nest (i.e., the nest was scanned from all directions). Once the trail was completed, the user returned to the starting point, the scanner was turned off, and data were saved for further analysis. After scanning, digital photos were taken for each nest from three different directions. These images were used during point cloud analysis to correct for any potential errors in the identification of the scanned nests (the point cloud does not allow for identifying the number from the flag; the flag can be misidentified because of random fallen branches present on the ground).

In the lab, data were downloaded and processed with the dedicated software (GeoSLAM Hub v.5.2.1, GeoSLAM Ltd., Nottingham, UK) to be transformed into "*.las*" files (laser format file, containing the LiDAR point cloud data) and "*.ply*" files (polygon format file containing the track of the scanning session in the field). The latter is important to see the order of the scanning process and identify nest numbers. These two types of files were later imported and processed in the CloudCompare open-source software, version 2.6.1 [37]. The software allows for computing local coordinates for individual points determined by the user (in our case, the tip of the red flag from each nest) (Figure 2). After placing points on all flags, the computed coordinates were saved in a text file (*.txt*).

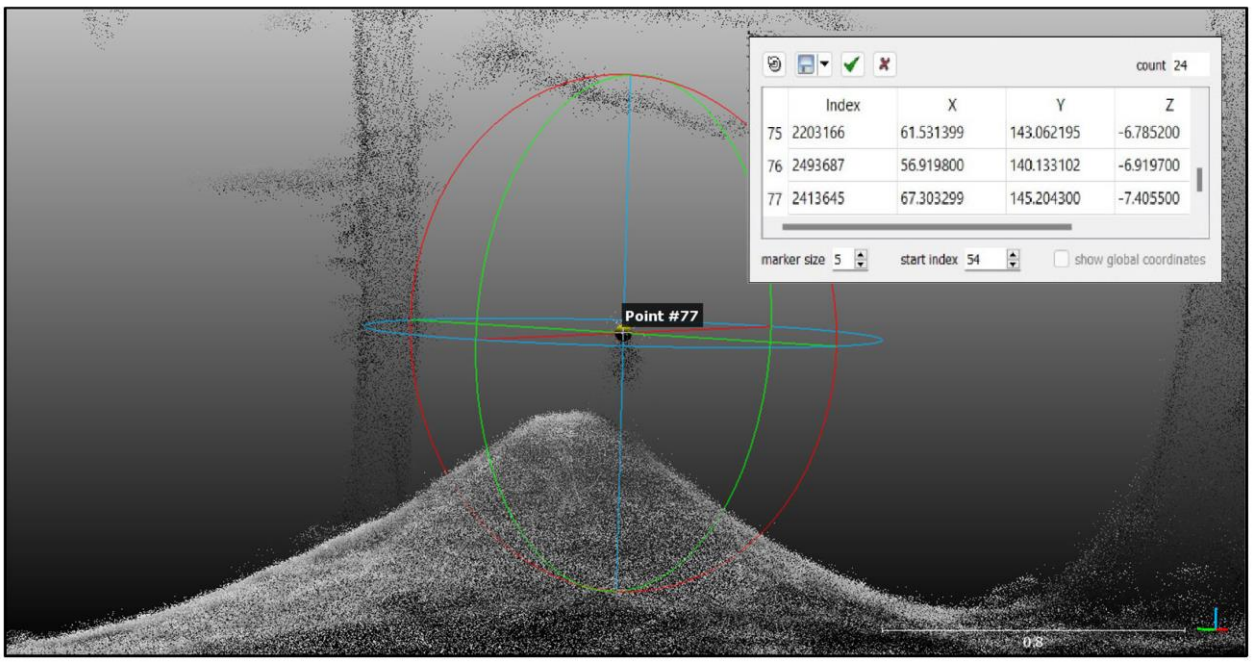

Figure 2. A nest obtained from a point cloud collected by MLS. In the center, the point at the tip of the flag placed on a nest for which the coordinates were determined in Cloud Compare (and shown in table from the upper right corner).

2.3. Data Analysis

The coordinates of MLS points are typically not georeferenced. As a result, analyses were carried out separately for each of the two types of sets, computing the distances among nests. Later, for each pair of nests in a set, the differences between the results of the two instruments were assessed. Analyses were carried out in QGIS 3.4 [38] and Microsoft Excel (2022) [39].

For datasets collected with the MLS (not having a geographical information), some preanalysis was required. First, a comma-separated value ("*.csv"*) data format was uploaded using the "*Add delimited text layer*" function (with the option "*point coordinates*" for the "*geometry definition*" field). A metric coordinate system (Stereo 70) was associated with the point cloud, and the result was saved as a shapefile format (*.shp*) for analysis. Further, as points from both instruments (GNSS and MLS) had spatial coordinates, they were uploaded into QGIS to compute the distances between pairs of nests in each dataset. This step was performed using the "*Distance Matrix*" function. Each of the 14 resulting datasets (two for each of the seven sets of ant nests) was processed and saved as a *.csv*-type file, which later were transformed into Microsoft Excel files (*.xlsx*) for computations. For each of the seven ant nest sets, two separate datasets resulted—one based on the GNSS and another one on the MLS. To compare the two instruments (GNSS and MLS), the difference between distance values determined by them for the same pair of nests was computed. The computations were carried out using all possible distances between any two nests from a track and also separately for distances between subsequent nests in a track.

Although many times, the agreement between two methods was determined by using correlation (or even regression) as there is no functional relationship between the two (i.e., the two resulting values are not separate variables having a conditional relationship), the Bland–Altman procedure is preferred [40]. This method quantifies the agreement between two measurements (obtained by different instruments) when the true value is not known. In such a case, the differences between paired measurements (based on GNSS and MLS in our case) are plotted against their means. The tendency for one method to exceed the other is expressed as the mean difference or bias (considering the MLS as the reference instrument when compared with GNSS) and the variability around this tendency (by constructing limits of agreement (LoA) expressed as the standard deviation of the differences) [41]. The resulting plot shows the distribution of the differences between two measurements of the same item (on the Y axis is the value of the difference; on the X axis is the average of the two measurements). A bias (mean of the differences between MLS and GNSS-based measurements) different from zero will show that a GNSS-based method systematically overestimates (positive bias) or underestimates (negative bias). The limits of agreement (LoA) are built around this bias and show the limits of the interval of agreement that represents the 95% confidence interval of differences (i.e., the range described by ± 1.96 standard deviations from the mean difference or bias). The acceptable values for the LoA are to be determined a priori by the user, depending on the desired level of accuracy and the accepted risk (in case of errors). For this study, we used the maximum limits set by the GNSS technical specifications (± 10 m, [33]) as measurements were made under closed canopy conditions. If most of the differences fall within this interval, the GNSS can be used as intended. Taking into account these advantages, the differences between the two tools used (GNSS vs. MLS) for the ant nest positioning were analyzed with the Bland–Altman method in the R software [42]. For each Bland–Altman plot, we also tested the correlation to find whether the bias depends on the size of the distance between nests.

We further investigated the potential differences between the two instruments in terms of the size and shape of the area determined by the nests. For these two variables, we used the convex polygon, including all points from one set. This was calculated in QGis (with the *Convex hull* function under the *Minimum bounding geometry* tool). Area and perimeter were used to assess the size and shape of the 14 polygons resulting from the point datasets. For shape analysis, the shape compactness (calculated as the ratio of the area of the polygon

to its squared perimeter, [43]) and form factor (calculated as the ratio of the area of the polygon and the area of the circumscribed circle, [44]) were computed.

To better understand the differences between GNSS- and MLS-based measurements, we also analyzed terrain configuration and canopy density as potential factors affecting the GNSS signal reception quality. We analyzed the terrain configuration using a digital elevation model (DEM) with an accuracy of 1 m (derived from the 1975 topographical map 1:25,000 [45]). The stand canopy density was analyzed using an enhanced vegetation index (EVI) image as a proxy. The image was derived from a modified Copernicus Sentinel 2 satellite image (2018) processed by Sentinel Hub (https://www.sentinel-hub.com (accessed on 5 October 2022)).

3. Results

3.1. Measuring Distances

The mean difference (i.e., bias) between GNSS and MLS-based distances was negative for most datasets with only four exceptions (out of the 14 datasets) (Table 1). The mean of biases over all datasets was −1.0 m, and the standard deviation was 1.6 m. Therefore, on average, the GNSS produced shorter distances between ant nests. Considering only the distances between consecutive nests, the mean of biases was smaller (−0.7 m) compared with distances between any two nests in no defined order (−1.4 m). The large standard deviation showed that differences were not very consistent either. The variation of biases was also smaller (SD = 0.8 m) when considering distances between consecutive nests (compared with SD = 2.2 m for differences between all possible distances). Consequently, the intervals of agreement (IoA) were also slightly smaller for consecutive nest distances (the mean of IoA was 14.3 m, compared with a mean of 19.0 m for all possible distances between nests).

Table 1. Results of the Bland–Altman analysis for the separate sets of nests included in the study ("all"—all possible distances between any two nests; "consecutive"—only distances between consecutive nests along the track; LoA—limits of agreement; IoA—interval of agreement; no. of dist.—number of distances between two nests).

Site	Set No. (No. of Nests)	Set Type	No. of Dist.	Bland–Altman			
				Bias (m)	LoA (m)		IoA (m)
					Inf.	Sup.	
Site 1	Set 1 (14 nests)	All	91	0.3	7.6	−6.9	14.5
		Consecutive	13	−0.5	4.9	−5.9	10.9
	Set 2 (30 nests)	All	435	−2.2	7.3	−11.7	19.0
		Consecutive	29	−0.3	7.0	−7. 6	14.6
	Set 3 (35 nests)	All	595	−1.5	7.3	−10.3	17.7
		Consecutive	34	0.3	8.5	−7.9	16.4
	Set 4 (41 nests)	All	820	−5.2	10.6	−20.9	31. 6
		Consecutive	40	−2.2	6.8	−11.2	18.1
Site 2	Set 5 (22 nests)	All	231	−2.4	5.7	−10.5	16.3
		Consecutive	21	−1.2	6.3	−8.6	14.9
	Set 6 (32 nests)	All	496	1.5	10.7	−7.7	18.4
		Consecutive	31	−1.0	6.3	−8.4	14.7
	Set 7 (35 nests)	All	595	−0.3	7.7	−8.2	15.9
		Consecutive	34	0.1	5.3	−5.2	10.5

The largest bias occurred for dataset 4, which also included the largest number of nests. The limits of agreement (LoA) were within the GNSS accuracy range (±10 m) with only one exception (set 4, for which also the highest mean difference was recorded).

For the consecutive distances, the differences between GNSS and MLS were not significantly affected by the size of the distance. The *p*-values of the slope in Figure 3 indicate that the slope was not significantly different from zero, and therefore, the trend was not significant. Moreover, in terms of the trend direction (orientation of the regression line), all possible variants were present: ascending (sets 1 and 2), descending (sets 4 and 7), and relatively stable (sets 3, 5, and 6).

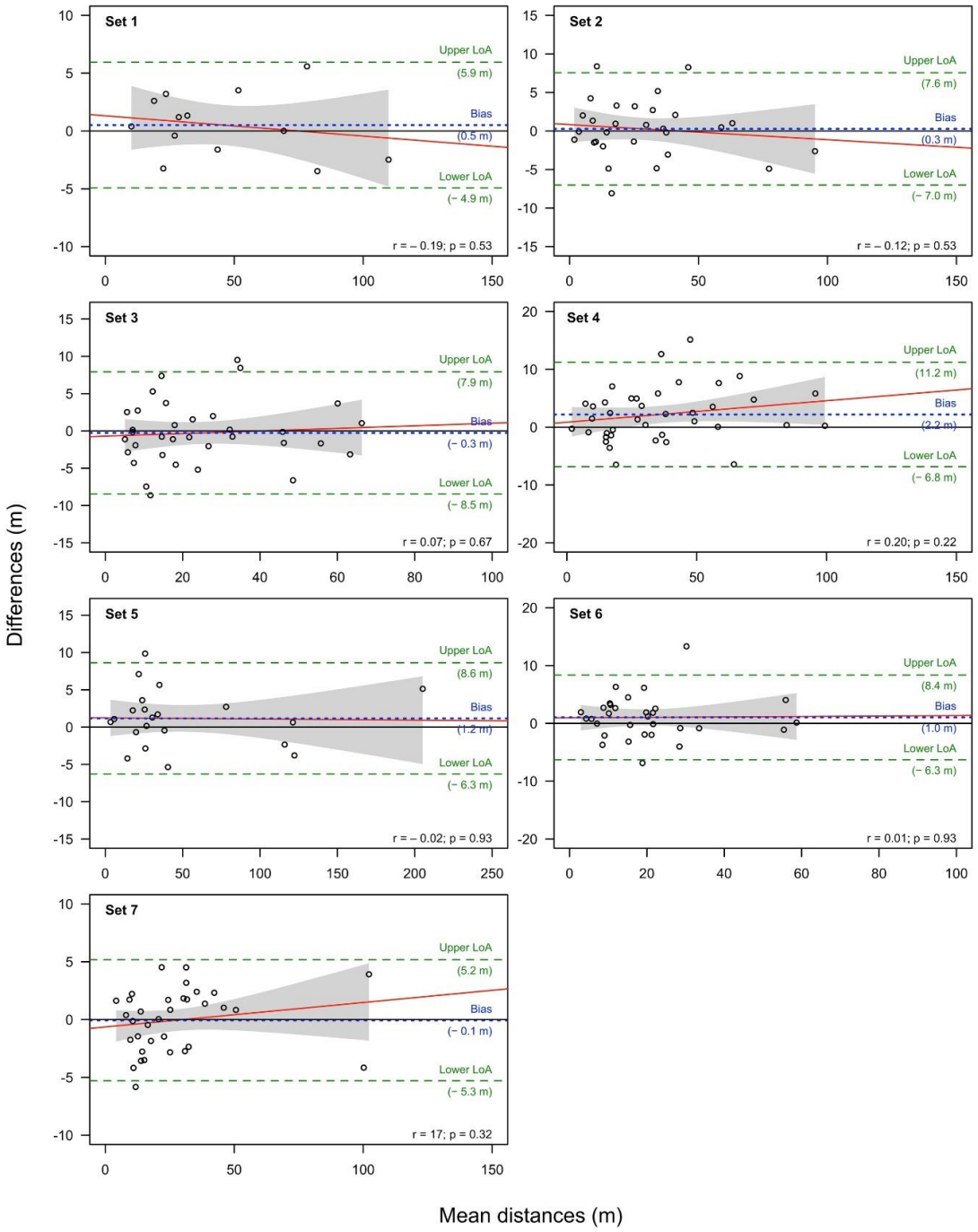

Figure 3. Results of the Bland–Altman analysis and linear regression for the datasets, including distances between subsequent points (nests). Note: the red line shows the regression between bias and mean differences.

However, for the set including all possible distances, the differences between GNSS and MLS-based distances depended significantly on the size of the distance itself, for five out of seven datasets. The linear regression showed a significant slope (i.e., trend) for datasets 1, 3, 4, 5, and 6 and a nonsignificant slope for datasets 2 and 7 (Figure 4). Nevertheless, when the trend was significant, the direction of the relationship was not consistent; increasing the distance, the differences between GNSS and MLS-based distances have increased for datasets 1 and 6, while the opposite trend was observed for datasets 3, 4, and 5.

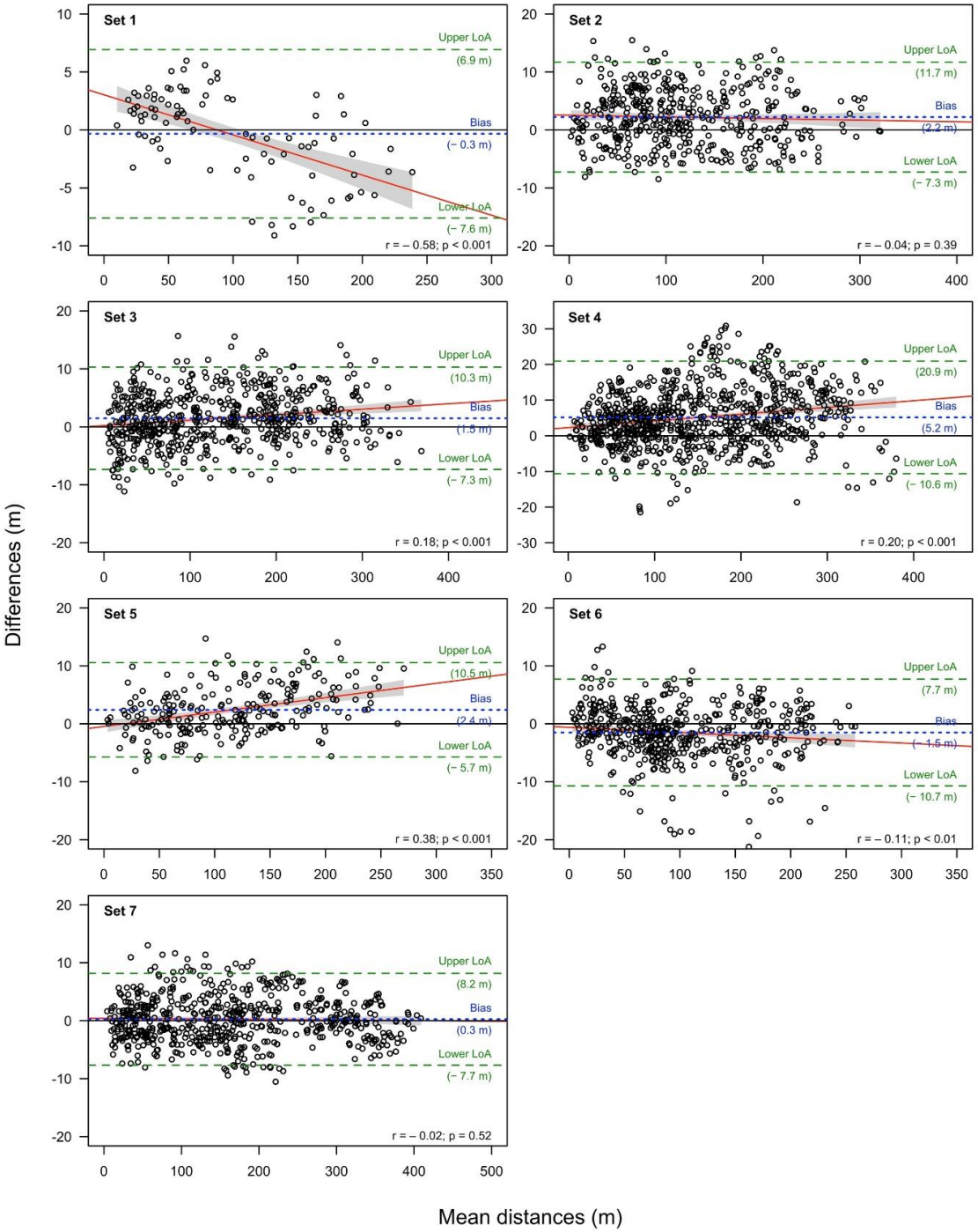

Figure 4. Results of the Bland–Altman analysis and linear regression for the datasets, including all distances between points (nests). Note: the red line shows the regression between bias and mean differences.

Results for the perimeter of convex hulls showed again no consistent trend (differences were positive and negative) and a rather small difference between the two instruments (Table 2). Dataset 4 showed again the largest difference, the perimeter of the shape determined by the GNSS being with 2.5% smaller than that based on MLS.

Table 2. The absolute and relative differences between perimeters based on GNSS and MLS. The relative differences were calculated as absolute difference divided by MLS-based perimeter and multiplied by 100.

Site	Dataset	Perimeter (in m), Based on		Absolute Diff. (m)	Rel. Diff. (%)
		MLS	GNSS		
#1	1	515.6	517.7	2.1	0.4
	2	740.4	734.9	−5.5	−0.7
	3	793.3	789.6	−3.7	−0.5
	4	974.8	950.1	−24.7	−2.5
#2	5	714.0	704.2	−9.8	−1.4
	6	614.4	616.7	2.3	0.4
	7	888.0	888.4	0.4	0.0

3.2. Measuring Areas and Shapes of Polygons

The area of the resulting convex polygons determined by GNSS was smaller in most cases (except for datasets 6 and 7) (Table 3). The largest difference was recorded for dataset 3, for which mean differences over measured distances were not the highest (Table 1). There was no significant correlation between the size of the area and the size of the relative difference (Table 3). However, the size of the area itself seems to influence the size of bias, as suggested by the trend between bias and the size of the convex hull area (Figure A2E,F).

Table 3. The area of the convex hulls determined by the nests within the 14 datasets and the relative differences between the two instruments (GNSS vs. MLS).

Site	Nest Set	Area (in m^2), Based on		Rel. Diff. (%)
		MLS	GNSS	
#1	1	12,860.9	12,259.4	−4.7
	2	26,954.0	25,160.5	−6.6
	3	23,288.4	21,323.0	−8.4
	4	57,498.9	52,989.5	−7.8
#2	5	28,439.5	27,582.5	−3.0
	6	19,935.0	19,962.6	0.1
	7	29,327.2	29,705.8	1.3

Both the shape compactness and the form factor of the polygons, were generally smaller for the GNSS-based method compared with the MLS-based method (Table 4). The dataset showing the largest mean difference (dataset 4, Table 1) also showed the highest values for both shape compactness and form factor. However, for shape compactness and form factor, the differences for dataset 4 were not the largest. Overall, the differences for both, shape compactness and form factor, were lower than 10%. The scatter plots in Figure A2A–D suggest a strong positive trend between the bias and both shape compactness and form factor for all sets.

The DEM produced for the study area revealed that most nests were located on a relatively flat ground and only a few in areas with steep slopes (Figure 5). Nests from dataset 4 within area 1 (the one showing the largest bias; see Table 1) were located in diverse conditions. Some of them were placed in steep terrain areas (on the ridge of ravines or at the bottom of the slope) and also distributed on both sides of a ravine (walking with the GNSS to cross the ravine might have influenced the quality of the GNSS signal).

Table 4. The shape compactness and form factor of the convex hulls, including the points for the 14 datasets. Relative differences (diff.) between the two instruments are shown in percent.

Site	Set	Shape Compactness			Form Factor		
		Instrument		Diff. (%)	Instrument		Diff. (%)
		MLS	GNSS		MLS	GNSS	
#1	1	0.048	0.046	−4.2	0.29	0.27	−6.9
	2	0.049	0.047	−4.1	0.34	0.31	−8.8
	3	0.037	0.034	−8.1	0.22	0.20	−9.1
	4	0.061	0.059	−3.3	0.49	0.45	−8.2
#2	5	0.056	0.056	0.0	0.45	0.45	0.0
	6	0.053	0.052	−1.9	0.38	0.38	0.0
	7	0.037	0.038	2.7	0.22	0.23	4.5

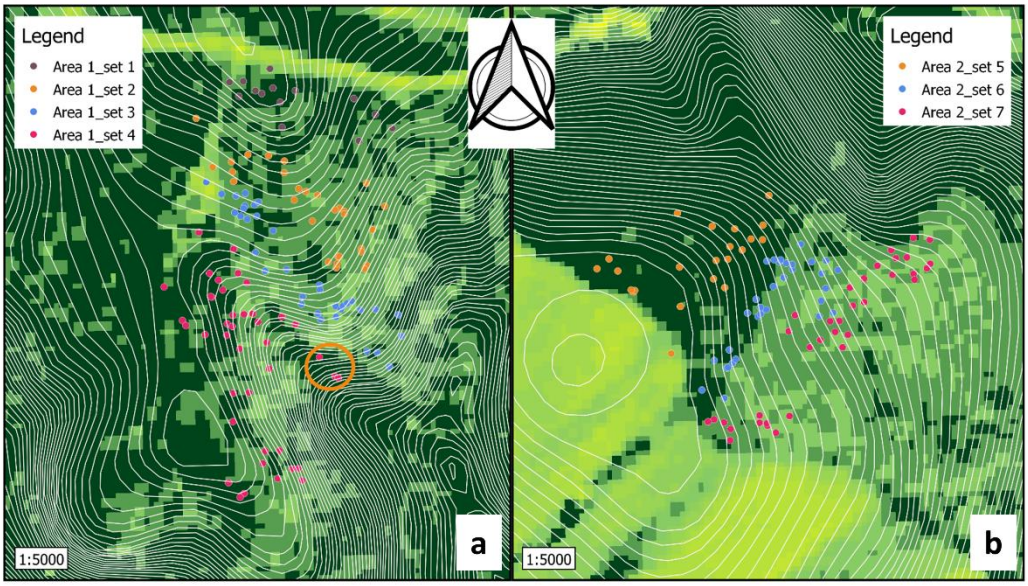

Figure 5. The terrain configuration revealed by the digital model and the canopy density revealed by the EVI classified image for the two analyzed areas (**a**—datasets 1 to 4; **b**—datasets 5 to 7). Nuances of green represent different canopy densities (with light green for open space and darkest green for fully closed dense canopy). The orange circle on the left image shows examples of nests located both under dense canopies and under steep terrain conditions.

4. Discussion

The differences between the two instruments are not necessarily surprising as each of them has a different methodology for producing location information. While the MLS is producing very large, continuous point data clouds in which points are linked to one another through other points (a path inside the cloud), the GNSS is recording location based on the information received from the satellites (independent of the location of other points). As the limits of agreement were, in general, less than the GNSS accuracy limits (±10 m), we can conclude that the GNSS provided reasonable measurements under forest canopy conditions. If this measurement accuracy is acceptable for the purpose of a study, GNSS seems a proper solution to use, having other important advantages, such as: (i) a more expedite use in the field, (ii) results carrying geographical information (coordinates) and can readily (without any complex processing) be used in a dedicated software program to compare their spatial distribution to other elements (such as stand boundaries for silvicultural works); (iii) the acquisition price being very low compared with the MLS technique.

Despite all these advantages, the quality of the recorded location with the GNSS could be affected by various factors [23]. Among them, those related to satellite availability are leading to the so-called dilution of precision (DOP) [46,47]. Besides the number and geometry of satellites, which are both important, the continuous change in time of these two variables is also influencing the accuracy of GNSS measurements, producing a combined form of dilution named geometric dilution of precision (GDOP). This includes the position dilution of precision (PDOP, in vertical and horizontal directions) and the time dilution of precision (TDOP). In general, a higher number of available satellites [48] and a wider positioning [46] reduce the PDOP. Additionally, ensuring enough position fixes per point improves the accuracy of GPS instruments [23]. However, other obstacles (e.g., dense canopies, clouds, tree stems, terrain configuration—ravines, canyons) can obstruct the reception of the GNSS receiver's antenna and impair the quality of the results even if the other proper conditions mentioned above are met [48]. Among all these, the negative effects related to the geometry of the satellites (position, number) or the collection time could be reduced by spending more time in each point (to allow for enough position fixes per point [23] or to allow for a better satellite number and configuration). Improper weather (e.g., the presence of clouds) could be avoided by taking measurements under more favorable conditions, while the negative impact of dense canopies could be reduced (but only for deciduous forests) by recording locations during the leafless period. Unfortunately, the negative influence of other factors (e.g., the rough terrain configuration, the stem density, and sometimes even the dense canopy) cannot be avoided and could produce large differences between the results from different stands (or different portions of the same stand but with different canopy or stem densities or terrain configuration). This could be another explanation for the results found here as well (especially for the fact that measurements were taken during summer when leaves were fully developed). If such field conditions (and resulting large errors, larger than the a priori set acceptable limits) are prevalent, the use of GNSS is not recommended.

The significant trend shown in Figure 4 for five out of the seven sets, including all distances, would imply a strong relationship between the size of the difference and the mean distance between points. However, trends were not constant but sometimes contrasting, showing an increase in the size of the differences with increasing mean distance, a decrease, and also no change (i.e., nonsignificant).

The bias between subsequent points was low (between 0.1 and −2.2 m) and matched the GNSS measurement accuracy limits (±10 m). However, in the case of nonsubsequent points (see "all" distances case, Table 1) spread within a more balanced shape area (close to a circle), the errors between points increase substantially, showing a less precise spatial positioning. However, the GNSS positioning error around a certain point is independent of the errors around other points along the track. Therefore, the distance itself and the presence of any intermediary points along the track should not influence the positioning error of a certain point recorded in the field. However, the timing of the recording could be important as working conditions are changing (satellite number and distribution; cloudiness), as well as the location features (canopy density, stem density, and terrain configuration were not uniform in the forests). For points that are farther away from each other and/or in case of longer field recording sessions, the chance for such changes is increasing (while for subsequent points along the track, the same chance is smaller). Therefore, the time dimension and spatial heterogeneity seem to affect the GNSS positioning accuracy but not the MLS (not affected by the causes mentioned in the case of GNSS).

The particular case of dataset 4, where the bias was larger than for the other datasets (for both cases, "consecutive" and "all" distances) and also where the largest bias was recorded, is special. Such a large bias cannot be explained by the size of distances between points as other sets (with lower bias) included similar distances (Table 2). However, it seems that the shape combined with the size of the polygon (convex hull) encompassing the points might have an effect on the bias. The bias increased with shape compactness and form factor for all sets (not only for set 4), as shown in Figure A2. Unfortunately, as the

data collected by the MLS could not be concatenated in a single set (as the GNSS collected data), a general analysis across the entire set (or at least for the cumulated set in each of the two analyzed areas) was not possible. Therefore, a comparison between dataset 4 and another very large set (in terms of distances, area covered, and shape) was not possible in this study.

Despite this apparent link between the bias and the size and/or shape of the area, including the nests, the area itself is not expected to play a role since the GNSS is taking the position for each location based on the signal received from the satellites, not being influenced by previous locations or their number. Therefore, other factors are expected to explain this result. For example, the variability in time and/or space of the environmental factors influencing the GNSS accuracy might be a more realistic explanation for the differences between the two instruments. The longer time needed to cover larger and/or more balanced areas increases the chance for changes in working conditions (such as weather (cloudiness) or the positioning system (number of satellites, distribution on the sky)). Such large areas might also increase the chance for important changes in stand parameters (canopy and stem density) and/or terrain configuration, which in turn affect the measurements [19,23]. In addition, taking GNSS measurements on the move did not allow for an appropriate number of fixes per point, which would have ensured higher accuracy [23]. Moreover, in this case, the digital model of the terrain has proven that the area with the largest bias was also the area with the most variable ground conditions (from a flat ground to deep ravines). Some of the nests in the dataset were located indeed in areas close to ravines where changes in GNSS positioning accuracy were expected [23]. Additionally, changes in canopy and stem density are expected to play a role in GNSS accuracy as well [19]. The EVI image revealed diverse stand conditions, from very dense canopies to more open. However, for dataset 4, the locations of some nests were both near steep slopes and under dense canopies. For example, for nest nos. 90 and 91 (orange circle in Figure 5, at the base of a steep slope), the bias was very large (over 15 m in general, reaching a maximum of 30 m) for distances to several other points (108 to 120). Therefore, a synergy of these two conditions is possible and could explain a larger bias.

5. Conclusions

Under forest canopy conditions, the GNSS has generally underestimated the distances between ant nests. However, compared with the MLS-based distances, the limits of agreement were within the GNSS accuracy limits. Despite meeting the expected accuracy, the systematic underestimation of GNSS-based distances should be considered when deciding on the instrument to be used. In certain field conditions, such as dense canopy and rugged terrain, the likelihood of large systematic errors increases, and therefore, the use of GNSS in such conditions should be limited. Furthermore, the areas of derived convex polygons were also underestimated by the GNSS-based method. Therefore, a precise spatial arrangement is less likely with the regular GNSS unit, especially when conditions (satellite number and position, weather conditions, canopy, stand density, and terrain configuration) are not favorable. Despite that differences in the MLS are not very large, the decision to use the GNSS should be based on the acceptable accuracy level. Moreover, if deciding to use the MLS (i.e., when higher accuracy is required), scanning objects of a known geographical position along with the points of interest would allow later for precise spatial positioning and, therefore, would be an important step in the data acquisition. Additionally, in the case of large datasets that need to be divided for laser scanning, data collection with the MLS should allow for later concatenation (point clouds should overlap). If GNSS is to be used, to improve results as much as possible (i.e., control potential error sources), the operator should allow enough time for collecting enough number of position fixes per point (i.e., longer collection time) or for averaging more samples for a waypoint before registration. Data collection should take place in the best conditions: clear sky, leafless period, a large number of satellites available, and with a more balanced distribution. Any

particular variables (e.g., terrain configuration, crown, and stem density) that cannot be controlled should be considered and taken into account during analysis.

Author Contributions: Conceptualization, P.T.S., I.D. and M.P.; methodology, P.T.S., S.C.F. and M.P.; data analysis, P.T.S., S.C.F. and I.D.; field investigation, P.T.S., S.C.F. and M.P.; writing—original draft preparation, P.T.S., I.D., S.C.F. and M.P.; writing—review and editing, P.T.S., I.D., S.C.F. and M.P. All authors have read and agreed to the published version of the manuscript.

Funding: This research received no external funding.

Data Availability Statement: Not applicable.

Acknowledgments: The authors would like to thank Forest Design S.R.L. for the help in processing data collected with MLS and the advice on data analysis with the CloudCompare software. The help provided by Andreea Turtoi, Mihai Stancu, and Laurențiu Cif for data collection from the field is greatly appreciated. The authors are thankful for the access to field sites and data from forest management plans granted by the Domeniul Hangu Forest District. GNSS and MLS data were collected during the fieldwork for the dissertation thesis of the second author presented for a bachelor's degree at the Faculty of Silviculture and Forest Engineering, Transilvania University of Brasov, Romania, in 2019. The work conducted by M.P. was carried under PN19070204, a grant from the Romanian Ministry of Education and Research.

Conflicts of Interest: The authors declare no conflict of interest.

Appendix A

Figure A1. The two instruments used for measurements. Garmin GPSMap 60CSx (on the **left**) and GeoSLAM-Zeb-Revo (on the **right**).

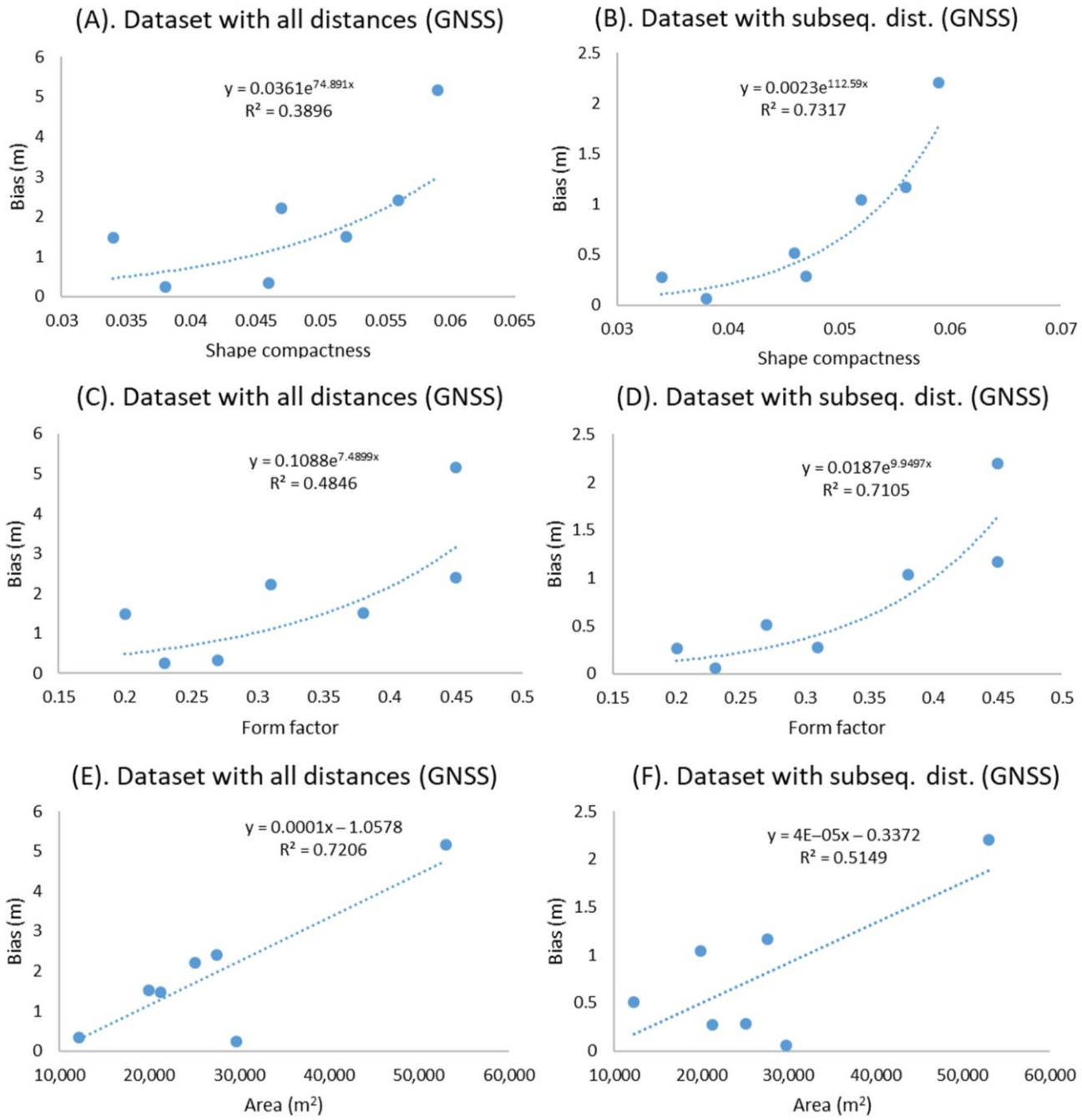

Figure A2. Scatter plots showing the influence of shape compactness (**A**,**B**), form factor (**C**,**D**), and area of the convex hull encompassing the points recorded by GNSS (**E**,**F**) on the mean difference between the two instruments (bias). Plots were drawn for both cases—bias determined in the case of distances between all points in a dataset (**A**,**C**,**E**) and distances between subsequent points in a dataset (**B**,**D**,**F**). (blue dots represent the observations; the regression line is represented by the dotted blue line).

References

1. Liang, X.; Kankare, V.; Hyyppä, J.; Wang, Y.; Kukko, A.; Haggrén, H.; Yu, X.; Kaartinen, H.; Jaakkola, A.; Guan, F.; et al. Terrestrial Laser Scanning in Forest Inventories. *ISPRS J. Photogramm. Remote Sens.* **2016**, *115*, 63–77. [CrossRef]
2. Hopkinson, C.; Lovell, J.; Chasmer, L.; Jupp, D.; Kljun, N.; van Gorsel, E. Integrating Terrestrial and Airborne Lidar to Calibrate a 3D Canopy Model of Effective Leaf Area Index. *Remote Sens. Environ.* **2013**, *136*, 301–314. [CrossRef]
3. Seidel, D.; Fleck, S.; Leuschner, C. Analyzing Forest Canopies with Ground-Based Laser Scanning: A Comparison with Hemispherical Photography. *Agric. For. Meteorol.* **2012**, *154–155*, 1–8. [CrossRef]

4. Van der Zande, D.; Stuckens, J.; Verstraeten, W.W.; Mereu, S.; Muys, B.; Coppin, P. 3D Modeling of Light Interception in Heterogeneous Forest Canopies Using Ground-Based LiDAR Data. *Int. J. Appl. Earth Obs. Geoinf.* **2011**, *13*, 792–800. [CrossRef]
5. Bayer, D.; Seifert, S.; Pretzsch, H. Structural Crown Properties of Norway Spruce (Picea Abies [L.] Karst.) and European Beech (Fagus Sylvatica [L.]) in Mixed versus Pure Stands Revealed by Terrestrial Laser Scanning. *Trees-Struct. Funct.* **2013**, *27*, 1035–1047. [CrossRef]
6. Lau, A.; Bentley, L.P.; Martius, C.; Shenkin, A.; Bartholomeus, H.; Raumonen, P.; Malhi, Y.; Jackson, T.; Herold, M. Quantifying Branch Architecture of Tropical Trees Using Terrestrial LiDAR and 3D Modelling. *Trees-Struct. Funct.* **2018**, *32*, 1219–1231. [CrossRef]
7. Kankare, V.; Holopainen, M.; Vastaranta, M.; Puttonen, E.; Yu, X.; Hyyppä, J.; Vaaja, M.; Hyyppä, H.; Alho, P. Individual Tree Biomass Estimation Using Terrestrial Laser Scanning. *ISPRS J. Photogramm. Remote Sens.* **2013**, *75*, 64–75. [CrossRef]
8. Liang, X.; Kankare, V.; Yu, X.; Hyyppä, J.; Holopainen, M. Automated Stem Curve Measurement Using Terrestrial Laser Scanning. *IEEE Trans. Geosci. Remote Sens.* **2014**, *52*, 1739–1748. [CrossRef]
9. Fortin, M.-J.; Dale, M.R.T.; ver Hoef, J. Spatial Analysis in Ecology. In *Encyclopedia of Environmetrics*; Piegorsch, W.W., El-Shaarawi, A.H., Eds.; John Wiley & Sons, Ltd.: Chichester, UK, 2002; pp. 2051–2058. ISBN 0471899976.
10. Hardy, O.J.; Sonké, B. Spatial Pattern Analysis of Tree Species Distribution in a Tropical Rain Forest of Cameroon: Assessing the Role of Limited Dispersal and Niche Differentiation. *For. Ecol. Manag.* **2004**, *197*, 191–202. [CrossRef]
11. Chen, X.; Li, B.L.; Scott, T.A.; Tennant, T.; Rotenberry, J.T.; Allen, M.F. Spatial Structure of Multispecies Distributions in Southern California, USA. *Biol. Conserv.* **2005**, *124*, 169–175. [CrossRef]
12. Seidler, T.G.; Plotkin, J.B. Seed Dispersal and Spatial Pattern in Tropical Trees. *PLOS Biol.* **2006**, *4*, e344. [CrossRef] [PubMed]
13. Zas, R. Iterative Kriging for Removing Spatial Autocorrelation in Analysis of Forest Genetic Trials. *Tree Genet. Genomes* **2006**, *2*, 177–185. [CrossRef]
14. Ferguson, A.W.; Klukowski, Z.; Walczak, B.; Clark, S.J.; Mugglestone, M.A.; Perry, J.N.; Williams, I.H. Spatial Distribution of Pest Insects in Oilseed Rape: Implications for Integrated Pest Management. *Agric. Ecosyst. Environ.* **2003**, *95*, 509–521. [CrossRef]
15. Birkhofer, K.; Henschel, J.R.; Scheu, S. Spatial-Pattern Analysis in a Territorial Spider: Evidence for Multi-Scale Effects. *Ecography* **2006**, *29*, 641–648. [CrossRef]
16. Moody, A.L.; Thompson, W.A.; De Bruijn, B.; Houston, A.I.; Goss-Custard, J.D. The Analysis of the Spacing of Animals, with an Example Based on Oystercatchers During the Tidal Cycle. *J. Anim. Ecol.* **1997**, *66*, 615–628. [CrossRef]
17. Vastaranta, M.; Melkas, T.; Holopainen, M.; Kaartinen, H.; Hyyppä, J.; Hyyppä, H. Laser-Based Field Measurements in Tree-Level Forest Data Acquisition. *Photogramm. J. Finl.* **2009**, *21*, 51–61.
18. Oveland, I.; Hauglin, M.; Gobakken, T.; Næsset, E.; Maalen-Johansen, I. Automatic Estimation of Tree Position and Stem Diameter Using a Moving Terrestrial Laser Scanner. *Remote Sens.* **2017**, *9*, 350. [CrossRef]
19. Sigrist, P.; Coppin, P.; Hermy, M. Impact of Forest Canopy on Quality and Accuracy of GPS Measurements. *Int. J. Remote Sens.* **1999**, *20*, 3595–3610. [CrossRef]
20. Magiera, W.; Vārna, I.; Mitrofanovs, I.; Silabrieds, G.; Krawczyk, A.; Skorupa, B.; Apollo, M.; Maciuk, K. Accuracy of Code GNSS Receivers under Various Conditions. *Remote Sens.* **2022**, *14*, 2615. [CrossRef]
21. Abdi, O.; Uusitalo, J.; Pietarinen, J.; Lajunen, A. Evaluation of Forest Features Determining GNSS Positioning Accuracy of a Novel Low-Cost, Mobile RTK System Using LiDAR and TreeNet. *Remote Sens.* **2022**, *14*, 2856. [CrossRef]
22. Næsset, E.; Jonmeister, T. Assessing Point Accuracy of DGPS Under Forest Canopy Before Data Acquisition, in the Field and after Postprocessing. *Scand. J. For. Res.* **2002**, *17*, 351–358. [CrossRef]
23. Deckert, C.; Bolstad, P. V Forest Canopy, Terrain, and Distance Effects on Global Positioning System Point Accuracy. *Photogramm. Eng. Remote Sens.* **1996**, *62*, 317–321.
24. Chen, Y.H.; Robinson, E.J.H. The Relationship between Canopy Cover and Colony Size of the Wood Ant *Formica Lugubris*—Implications for the Thermal Effects on a Keystone Ant Species. *PLoS ONE* **2014**, *9*, e116113. [CrossRef] [PubMed]
25. Procter, D.S.; Cottrell, J.; Watts, K.; Robinson, E.J.H. Do Non-Native Conifer Plantations Provide Benefits for a Native Forest Specialist, the Wood Ant *Formica Lugubris*? *For. Ecol. Manag.* **2015**, *357*, 22–32. [CrossRef]
26. Sudd, J.H.; Douglas, J.M.; Gaynard, T.; Murray, D.M.; Stockdale, J.M. The Distribution of Wood-Ants (*Formica Lugubris Zetterstedt*) in a Northern English Forest. *Ecol. Entomol.* **1977**, *2*, 301–313. [CrossRef]
27. Gibb, H.; Andersson, J.; Johansson, T. Foraging Loads of Red Wood Ants: *Formica Aquilonia* (Hymenoptera: Formicidae) in Relation to Tree Characteristics and Stand Age. *PeerJ* **2016**, *4*, e2049. [CrossRef]
28. Kadochová, Š.; Frouz, J. Red Wood Ants *Formica Polyctena* Switch off Active Thermoregulation of the Nest in Autumn. *Insectes Soc.* **2014**, *61*, 297–306. [CrossRef]
29. Punttila, P.; Kilpeläinen, J. Distribution of Mound-Building Ant Species (*Formica* spp., *Hymenoptera*) in Finland: Preliminary Results of a National Survey. *Ann. Zool. Fenn.* **2009**, *46*, 1–15. [CrossRef]
30. Schreiber, U.; Brennholt, N.; Simon, J. Gas Permeable Deep Reaching Fracture Zones Encourage Site Selection of Ants. *Ecol. Indic.* **2009**, *9*, 508–517. [CrossRef]
31. FMP. *Forest Management Plan for the Production Unit No. I Codrii Paşcanilor—Sturdza*; Terra Rosa Proiect S.R.L.: Tartaresti, Romania, 2013.
32. Fick, S.E.; Hijmans, R.J. WorldClim 2: New 1-km Spatial Resolution Climate Surfaces for Global Land Areas. *Int. J. Climatol.* **2017**, *37*, 4302–4315. [CrossRef]

33. Garmin Ltd. GPSMAP 60Csx Owner's Manual. Available online: https://static.garmin.com/pumac/GPSMAP60CSx_OwnersManual.pdf (accessed on 5 October 2022).
34. GeoSLAM Ltd. ZEB_Revo Specifications Sheet. Available online: https://geoslam.com/wp-content/uploads/2021/03/ZEB_Revo_Spec_Sheet.pdf (accessed on 5 October 2022).
35. Neudam, L.; Annighöfer, P.; Seidel, D. Exploring the Potential of Mobile Laser Scanning to Quantify Forest Structural Complexity. *Front. Remote Sens.* **2022**, *3*. [CrossRef]
36. GeoSLAM Ltd. ZEB_Revo User's Manual. Available online: https://download.geoslam.com/docs/zeb-revo/ZEB-REVOUserGuideV3.0.0.pdf (accessed on 5 October 2022).
37. CloudCompare-3D Point Cloud and Mesh Processing Software, Version 2.6.1. 2015. Available online: http://www.danielgm.net/cc/ (accessed on 17 December 2018).
38. OSGeo, QGIS 3.4—QGIS Geographic Information System 2019. Available online: https://qgis.org/en/site/ (accessed on 20 January 2019).
39. Microsoft Corporation. Excel vers. 16.66.1. Available online: https://office.microsoft.com/excel.
40. Giavarina, D. Understanding Bland Altman Analysis Lessons in Biostatistics. *Biochem. Medica* **2015**, *25*, 141–151. [CrossRef] [PubMed]
41. Bland, J.M.; Altman, D.G. Measuring Agreement in Method Comparison Studies. *Stat. Methods Med. Res.* **1999**, *8*, 135–160. [CrossRef]
42. R Core Team. *R: A Language and Environment for Statistical Computing*; R Foundation for Statistical Computing: Vienna, Austria, 2017.
43. Bogaert, J.; Rousseau, R.; Van Hecke, P.; Impens, I. Alternative Area-Perimeter Ratios for Measurement of 2D Shape Compactness of Habitats. *Appl. Math. Comput.* **2000**, *111*, 71–85. [CrossRef]
44. Haggett, P. *Locational Analysis in Human Geography*; St. Martin's: London, UK, 1966.
45. DTM. *Romania Harta Topografică, Scara 1:25000*; Direcția Topografică Militară: Bucharest, Romania, 1977.
46. Januszewski, J. Sources of Error in Satellite Navigation Positioning. *TransNav, Int. J. Mar. Navig. Saf. Sea Transp.* **2017**, *11*, 419–423. [CrossRef]
47. Pattanayak, B.; Moharana, L. Analyzing the Effect of Dilution of Precision on the Performance of GPS System. In Proceedings of the 1st Odisha International Conference on Electrical Power Engineering, Communication and Computing Technology (ODICON), Bhubaneswar, India, 8–9 January 2021. [CrossRef]
48. Langley, R.B. Dilution of Precision. *GPS World* **1999**, *10*, 52–59.